Does the severity of non-flow periods influence ecosystem structure and function of temporary streams? A mesocosm study

Isabel Muñoz[1] | Meritxell Abril[1] | Joan Pere Casas-Ruiz[2] | Maria Casellas[2] | Lluís Gómez-Gener[1] | Rafael Marcé[2] | Margarita Menéndez[1] | Biel Obrador[1] | Sergi Sabater[2,3] | Daniel von Schiller[2,4] | Vicenç Acuña[2]

[1]Department of Evolutionary Biology, Ecology and Environmental Sciences, University of Barcelona, Barcelona, Spain

[2]Catalan Institute for Water Research (ICRA), Girona, Spain

[3]Institute of Aquatic Ecology, University of Girona, Girona, Spain

[4]Faculty of Science and Technology, University of the Basque Country, Bilbao, Spain

Correspondence
Vicenç Acuña, Catalan Institute for Water Research (ICRA), Girona, Spain.
Email: vicenc.acuna@icra.cat

Abstract

1. Global change is dramatically altering flow regimes worldwide. Among the most important consequences are the transition of many permanent waterways to temporary waterways, the increase in duration and frequency of non-flow periods of temporary streams, and the increase in the severity (i.e. irradiance, temperature and humidity) of the non-flow period. Nowadays, there is a lack of knowledge on how changes in duration, frequency and severity of the non-flow period will reflect on biodiversity and biogeochemical changes in temporary streams.

2. We designed a manipulative experiment using artificial streams to evaluate the effects of severity of the non-flow period on stream biofilms. Sixteen artificial streams were assigned to four treatments: continuous flow, continuous intermittency and intermittency with and without rain events. Effects were assessed on selected features of stream biofilm structure (i.e. bacterial density and basal fluorescence) and function (photosynthetic efficiency and enzymatic activities), as well as CO_2 emissions and dissolved organic matter quantity and quality from water column and sediments.

3. The occurrence of rain events during the non-flow period enhanced organic carbon processing and CO_2 emissions to the atmosphere, reducing the sediment reservoir of exportable organic carbon and therefore reducing the dissolved organic carbon exports from streambeds at flow resumption. Given the ongoing reducing trends in the frequency of rain events in semi-arid and arid regions, we expect temporary streams to process and emit less and to export more carbon to downstream systems.

KEYWORDS
CO_2 emissions, flow intermittency, organic carbon, stream biofilm, temporary streams

1 | INTRODUCTION

Temporary streams and rivers, defined as waterways that cease to flow at some points in space and time along their course (Acuña et al., 2014), are a dominant landscape freshwater feature in many regions of the globe (Raymond et al., 2013). Their number is expected to increase in the light of climate change and by increasing withdrawal of freshwater resources (Pekel, Cottam, Gorelick, & Belward, 2016). Despite the increase in studies on temporary waterways over the past decade, the comprehension of the relationship between flow regime components and the ecosystem structure and function remains limited (Acuña et al., 2014). Among the most relevant and certainly distinctive components of the flow regime in temporary waterways, we found those characterising the dry phase (or non-flow periods). Specifically, the non-flow periods can be characterised by a series of spatial (i.e. location and extension of dry reaches) and temporal (i.e. frequency, duration and predictability) components. Many studies have assessed the relevance of the spatial components on biodiversity (Bogan, Boersma, & Lytle, 2013; Davis, Pavlova, Thompson, & Sunnucks, 2013; Hermoso, Ward, & Kennard, 2013), and some assessed the relevance of the temporal components on biodiversity (Febria, Hosen, Crump, Palmer, & Williams, 2015; Garcia, Gibbins, Pardo, & Batalla, 2017; Schriever et al., 2015; Stubbington, Gunn, Little, Worrall, & Wood, 2016); however, few have assessed the relevance of these components on function (Acuña, Casellas, Corcoll, Timoner, & Sabater, 2015). Regardless of the considered ecological response variables, to date, no studies have considered the severity of the non-flow period, here understood as the conditions experienced by biological communities during the non-flow period in terms of humidity, temperature and irradiance. For example, the streambed temperature of a floodplain experiencing the same duration of the non-flow period might range from 20 to 40°C in a few metres along the course of a stream channel (Tonolla, Acuña, Uehlinger, Frank, & Tockner, 2010), and these differences might profoundly affect biological communities (Indermaur, Schmidt, Tockner, & Schaub, 2010) and biogeochemical processes (Doering, Uehlinger, Ackermann, & Woodtli, 2011). Less understood is the effect of sediment humidity, which is determined by the sediment type, the vertical hydrologic connection with ground water, the riparian cover and rainfall events.

Rainfall events are known to stimulate biological and biogeochemical activities for short times, but their influence might continue beyond the duration of the rain events. There are many studies reporting effects of rain events on soil sediment function. For example, size, intensity and sequence of rain events in space and time determined the fate of available nitrogen and carbon (Borken & Matzner, 2009; Welter, Fisher, & Grimm, 2005) and their processing mechanisms. Another study analysing the functional diversity of soil microorganisms affected by dry periods observed that their capacity to degrade different organic carbon sources increased in soils sporadically exposed to rain events compared with soils permanently exposed to dry conditions (Williams & Rice, 2007). Given the fast response of stream biofilms to flow recovery (Amalfitano et al., 2008; Timoner, Borrego, Acuña, & Sabater, 2014) and to rewetting (Gallo, Lohse, Ferlin, Meixner, & Brooks, 2014; Timoner, Acuña et al., 2014), we expect changes in stream biofilms during and after rain events, likely influencing ecosystem function.

Overall, a better comprehension of the effects of each one of the temporal components of the non-flow phase (duration, frequency and predictability), as well as the severity of the non-flow phase, is needed to better understand the relationship between the natural flow regime and ecosystem structure and function of temporary streams. We believe this knowledge is currently crucial to anticipate changes by the ongoing climate change-driven increases in the magnitude and frequency of the non-flow periods, with most likely more severe conditions because of the overall decrease in the number of rain events (Polade, Pierce, Cayan, Gershunov, & Dettinger, 2014). Here, we designed a manipulative experiment using artificial streams to evaluate the effects of the severity of the non-flow period (as occurrence of rain-derived rehydration events during the non-flow period) on stream biofilm structure and function. We expected that the lower severity associated with rehydration events during the non-flow period would influence stream biofilms, so that biofilm structure would be less impaired by the non-flow conditions (1); biofilm function will increase immediately after the rehydration and at least partially persist during the non-flow period (2); and biofilm recovery at the end of the non-flow period would be quicker for those streams experiencing lower severity during the non-flow period (3).

2 | METHODS

2.1 | Experimental design

Experiments were conducted in a series of artificial streams located at the indoor Experimental Streams Facility of the Catalan Institute for Water Research (Girona, NE Iberian Peninsula). Each of the 16 artificial streams was assigned to one of four treatments following a randomised block design (with four replicates per treatment; and one replicate per block of four artificial streams). Specifically, there were two control treatments, namely one experiencing continuous flow throughout the whole experiment (colonisation and experimental phase) (F) and one experiencing non-flow conditions during the entire experimental phase (NF). The flow intermittency treatments differed regarding severity, as one experienced a severe non-flow period of 29 days (I), and one experienced a less severe non-flow period of 29 days because of a rehydration pulse emulating the effects of a rain event lasting 30 min, and accounting for 10 L/m^2 at day 21 (RH) (Figure 1). Non-flow and consequent streambed desiccation were simulated by avoiding water flow in the artificial streams and by allowing the stream substrata to air-dry at room temperature (c. 20°C). This approach implied that complete desiccation was achieved 7 days after the flow interruption, a time lapse similar to that observed in nearby temporary streams (Timoner, Acuña, von Schiller, & Sabater, 2012). The selected duration of the non-flow
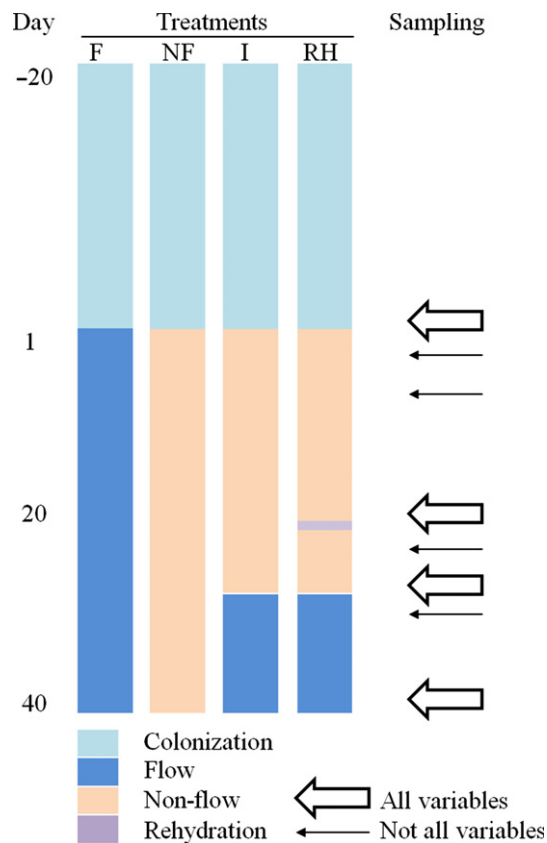
FIGURE 1 Experimental design and sampling schedule [Colour figure can be viewed at wileyonlinelibrary.com]

period represented a trade-off between the observed natural ranges of non-flow duration and those that can be properly tested in the artificial streams. Specifically, we simulated a non-flow period of 29 days, while the mean duration of the non-flow period of temporary streams and rivers in the region is 37 ± 43 days (Colls, Timoner, Sabater, & Acuña, 2018). The duration and intensity of the rain event at day 21 simulated a normal rainfall event, allowing only for a partial rehydration of streambed sediments that lasted ca. 2 days, although without surface water flow. Flow was restored at the end of the non-flow period and then maintained for another 14 days to allow recovery. The impact of the severity of the non-flow period on the resilience of stream biofilm structure and function was assessed by comparing the two flow intermittency treatments with the continuous flow and non-flow treatments after the non-flow period.

2.2 | Experimental conditions

Each artificial stream consisted of an independent methacrylate channel (200 cm long, 10 cm wide and 10 cm deep) and a 70-L water tank from which water was recirculated. Each stream received a constant flow of 50 ml/s and operated under a scheme of combined flow recirculation (118 min) and continuous flow (2 min) every 2 hr. The water exchange rate was 4.3% per hour, so the water of each artificial stream was completely renewed once a day. Mean water velocity was 0.88 ± 0.03 cm/s, and water depth over

the plane bed ranged between 2.2 and 2.5 cm. Each artificial stream was filled with 5 L of sandy sediment extracted from the upper 10 cm of an unpolluted segment of a nearby Mediterranean stream (Llémena River; NE Iberian Peninsula; sediment size percentile 50 = 0.74 mm). The sand was sterilised with a Presoclave-II 30 L autoclave (120°C for 2 hr; JP Selecta S.A., Barcelona, EU) and evenly distributed in the artificial streams to create a plane bed that facilitated the growth of biofilm. Once the sand was evenly distributed, the sediment depth in the artificial streams ranged between 5 and 5.5 cm, which would be representative of a relatively narrow hyporheic zone but approximately corresponded to the average depth of the sediments extracted from the Llémena River. At complete water saturation, the porosity of the sand yielded a water content of 24.3 ± 3.2% of the wet weight, assessed as the percentage of water weight of the sediment. Source water for the artificial streams was rainwater, filtered through activated carbon filters. Daily cycles of photosynthetically active radiation were defined as 12-hr daylight + 12-hr darkness and were simulated using LED lights (Lightech, Girona, Spain). Photosynthetically active radiation was held constant at 174 ± 33 $\mu Em^{-2} s^{-1}$ during the daytime and was recorded every 10 min using 4 quantum sensors located across the whole array of streams (sensor LI-192SA, LiCOR Inc, Lincoln, USA). Air temperature was maintained at 20°C during the experiment at an air humidity of 30%. Water temperature was recorded every 10 min using VEMCO Minilog (TR model, AMIRIX Systems Inc, Halifax, NS, Canada) temperature data loggers (−5 to 35°C, ± 0.2°C). Overall, the physicochemical conditions were designed to mimic the conditions of pristine Mediterranean streams during summer. Specifically, the selected duration of the daylight, the photosynthetically active radiation intensity and the water temperature simulated those of the Llémena River during late summer, when the sediments and the inocula from the river were extracted.

Biofilm colonisation was allowed in the artificial streams before the exposure to non-flow conditions. Biofilm was inoculated twice per week during the colonisation period using combined inocula from epilithic (growing on the surface of rocks) and epipsammic (growing on the surface of sand) biofilms of the Llémena River. During the colonisation period, biofilms were monitored twice per week for their effective photosynthetic yield (Y_{eff}). These measurements provided information on the physiological status of the biofilms in the artificial streams and were made to assess the physiological similarity between the biofilms colonising the artificial streams and the biofilms from the Llémena River and to assess the homogeneity between the artificial streams before the exposure to non-flow conditions. The colonisation period ended when biofilms in artificial streams achieved values of Y_{eff}, similar to those of the Llémena River (0.3–0.4), 5 weeks after the first inocula was added. Even though biofilms showed similar photosynthetic activity and biomass values similar to those of the Llémena River, the community complexity was not comparable to that of a natural river, as we excluded large consumers. This implies that the food-chain length was shorter in our artificial streams, therefore constraining the ecosystem response to the lower trophic levels.

2.3 | Water and sediment chemistry

The sediment water content was measured during the non-flow period, calculated as difference between the wet and dry weights of the samples (including both biofilm and substrata) after 24 hr at 110°C and expressed as the percentage of water of the wet weight. Dissolved oxygen, pH and specific conductivity were measured weekly at noon in each artificial stream using hand-held probes (WTW, Weilheim, Germany). Concentrations of nutrients and dissolved organic carbon (DOC) were measured weekly from water collected from the channel outlet. Water was immediately filtered through 0.7-μm glass fibre filters (Whatman GF/F, Kent, UK) into pre-washed polyethylene containers. The concentration of soluble reactive phosphorus (SRP) was determined colourimetrically using a fully automated Alliance Instruments Smartchem 140 (AMS, Frépillon, France) discrete analyser. The concentrations of $N-NO_3^-$ and $N-NH_4^+$ were determined on a Dionex ICS-5000 ion chromatograph (Dionex Corporation, Sunnyvale, USA). DOC was measured on a Shimadzu TOC-V CSH (Shimadzu Corporation, Kyoto, Japan).

Changes in the sediment water-extractable organic matter (WEOM) were assessed to characterise the effects of the different treatments on the organic matter quantity and quality in the sediment. WEOM is operationally defined as the water-soluble fraction of sediment organic matter recoverable through mild agitation with an aqueous solution and represents the most mobile and bioreactive fraction of sediment organic matter (Zsolnay, 1996). In our experiment, WEOM was extracted by shaking 30 g of sediment in Milli-Q water with a sediment: water ratio of 1:10 (w/w), and the extraction was carried out at 150 rpm and 4°C in a dark benchtop incubator (Excella E24 R, New Brunswick, Eppendorf, Germany). WEOM was quantified as water-extractable organic carbon after filtration through 0.7 μm glass fibre filters as described in the water column DOC. The composition of WEOM was assessed through fluorescence spectroscopy after filtration through 0.2 μm nylon filters (Whatman, UK). Fluorescence samples were analysed within 24 hr after collection as described in a previous study (Casas-Ruiz et al., 2017). In brief, we acquired excitation–emission matrices (EEMs) on a fluorescence spectrophotometer (F-7000, Hitachi, Japan) with a 1-cm quartz cuvette. Scans were collected over 3-nm increments for the excitation (248–449 nm) and the emission (250–550 nm) wavelengths. EEMs were blank subtracted, corrected for inner-filter effects and instrument-specific biases, and normalised to the Raman peak area. We then calculated: (1) the humification index (HIX; unitless) as the ratio between the peak area under the fluorescence emission spectra of 435–480 nm and 300–345 nm at an excitation wavelength of 254 nm (Zsolnay, Baigar, Jimenez, Steinweg, & Saccomandi, 1999); and (2) the biological index (BIX; unitless) as the ratio of the fluorescence intensity emitted at 380 and 430 nm for an excitation of 310 nm (Huguet et al., 2009). HIX values increase with the extent of DOM humification (Zsolnay et al., 1999), whereas BIX values positively correlate with the presence of fresh, recently produced DOM (Huguet et al., 2009; Wilson & Xenopoulos, 2009). These variables (WEOM, and its HIX and BIX values) were measured at specific days corresponding to the moments when any change in water flow was performed: 1 day before the non-flow period (−1 day), one day before the rainfall event (20 days), one day before the flow recovery (28 days) and at the end of the experiment (42 days).

2.4 | Biofilm structure and function

The response of biofilms to different treatments was assessed in terms of structure (basal fluorescence [F_0] and bacterial density) and function (Y_{eff}, alkaline phosphatase [APA] and leucine amino peptidase [LAP] activities). In all the cases, the estimates were performed in sediments obtained in each of the artificial streams at each sampling time with a sample corer of 1.2 cm in diameter, from which the uppermost 1 cm was considered for analysis. These variables were measured on the same days as WEOM, HIX and BIX, plus two additional dates in the case of bacterial density, LAP and APA: two hours after the rainfall event (21 days) and two days after flow recovery (31 days); and five additional dates in the case of F_0 and Y_{eff}: the 3 ones previously described for LAP and APA, plus days 1 and 2 (see details below).

The F_0 is the basal fluorescence of the algal component of the biofilm and can be used as an in vivo estimate of algal biomass (Schmitt-Jansen & Altenburger, 2008). This variable allows the evaluation of the algal response to environmental stressors (Corcoll et al., 2015). The F_0 was estimated for several ($n = 5$) sediment spots with a portable pulse amplitude modulate fluorometer (Diving-PAM; WALZ, Effeltrich, Germany), and the averaged value was provided as the F_0 of the channel. The Y_{eff} was also assessed with the Diving-PAM with the same procedure. This parameter reflects the energy conversion at Photosystem II reaction centres (Schreiber, Müller, Haugg, & Gademann, 2002) and is commonly used to evaluate the physiological state of primary producers and their response to different environmental stressors such as toxicants, light stress or desiccation (Corcoll et al., 2015).

Bacterial density was estimated after each sediment sample was sonicated for 90 s using a sonication bath (Selecta) operating at 40 W and 40 kHz. The sonicated supernatant was collected and a subsample stained using 4'-6'-diamidino-2-phenylindole (DAPI, Sigma-Aldrich). Samples were then filtered (0.2-μm pore-diameter black polycarbonate filters, Nucleopore, Whatman) and at least 20 fields were randomly counted by epifluorescence microscopy (Nikon Eclipse 80i; Nikon, Tokyo, Japan) in each slide. The results are presented as the number of bacterial cells per cm.

Two different extracellular enzyme activities were analysed in the epipsammic biofilms to account for their ability to degrade dissolved organic matter. The measured activities were related to the degradation capacity of N (leucine-aminopeptidase, LAP) and P organic compounds (alkaline phosphatase, APA). The extracellular enzyme activities were measured by means of fluorescent-linked substrates (methylumbelliferyl [MUF] for APA; and aminomethyl-coumarin [AMC] for LAP). Biofilm samples were again obtained after sonication of the sediments for 90 s using the sonicating bath described above. Suspended biofilms were then incubated for 1 hr

in the dark at 20°C immediately after each sampling. Incubations were performed at a final concentration of 300 μmol/L (determined saturation concentration for these communities (Romaní, Giorgi, Acuña, & Sabater, 2004). Blanks and standards of MUF and AMC (0–100 μmol/L were also incubated. At the end of the incubation, glycine buffer (pH = 10.4) was added (1/1 vol/vol), and the fluorescence was measured at 365/455 nm excitation/emission for MUF and at 364/445 nm excitation/emission for AMC. Values were expressed as μmoles MUF/AMC cm^{-2} h^{-1}.

2.5 | CO$_2$ fluxes

The net CO$_2$ flux between either the water or the sediment and the atmosphere was determined during daytime on the same days as when the other variables were measured (Figure 1). Additionally, CO$_2$ flux was intensively assessed along three specific moments: the non-flow phase, the rehydration pulse and the flow recovery (every 1–3 hr after the beginning of each event; Figure 1). The CO$_2$ flux between the water and the atmosphere (F_{CO_2}) was obtained by applying Fick's first law of gas diffusion:

$$F_{CO_2} = k_{CO_2} K_h \left(p_{CO_2,w} - p_{CO_2,a} \right) \tag{1}$$

where K_h (mmol μatm^{-1} m^{-3}) is Henry's constant for CO$_2$ adjusted for salinity and temperature (Millero, 1995; Weiss, 1974), $p_{CO_2,w}$ (μatm) and $p_{CO_2,a}$ (μatm) are the mean partial pressures of CO$_2$ in surface water and air, respectively, and the k_{CO_2} (m/day) is the specific gas transfer velocity for CO$_2$. Positive values of F_{CO_2} represent gas efflux from the water to the atmosphere, and negative values indicate gas influx from the atmosphere to the water.

The $p_{CO_2,w}$ and $p_{CO_2,a}$ were measured at the outlet of the channels with an infrared gas analyser (EGM-4, PP-Systems, USA). For $p_{CO_2,w}$ measurements, the water samples were circulated through a membrane contactor (MiniModule, Liqui-Cel, USA) coupled to the gas analyser (Teodoru, Prairie, & del Giorgio, 2011) at 300 mL/min. The measurement accuracy of the EGM-4 is estimated to be within 1% over the calibrated CO$_2$ range.

The k_{CO_2} was obtained based on the decline in dissolved propane (C$_3$H$_8$) concentrations during steady state injections of propane and Cl$^-$ as a conservative tracer (Genereux & Hemond, 1992). We corrected the $k_{C_3H_8}$ for depth to obtain the mean gas transfer velocity of propane (Raymond et al., 2012), and we further transformed it to k_{CO_2} by applying Equation 2:

$$k_{CO_2} = k_{C_3H_8} \left(\frac{Sc_{CO_2}}{Sc_{C_3H_8}} \right)^{-n} \tag{2}$$

where $k_{C_3H_8}$ is the mean gas transfer velocity of C$_3$H$_8$ (m/day), Sc_{CO_2} is the Schmidt number of CO$_2$ at a given water temperature (Wanninkhof, 1992), and $Sc_{C_3H_8}$ is the Schmidt number of C$_3$H$_8$ at a given water temperature. We set the exponent n to 1/2 for turbulent environments, that is, flowing waters (Bade, 2009).

The CO$_2$ flux between the dry sediments and the atmosphere (F_{CO_2}) was obtained by applying the enclosed chamber method (Livingston & Hutchinson, 1995). Briefly, we monitored the gas concentration in an opaque chamber every 4.8 s with an infrared gas analyser (EGM-4, PP-Systems, USA). Measurement accuracy of the EGM-4 is estimated to be within 1% over the calibrated range. In all the cases, flux measurements lasted until a change in CO$_2$ of at least 10 μatm was reached, with a maximum duration of 300 s and a minimum of 120 s. We calculated the F_{CO_2} (mmol m^{-2} day^{-1}) from the rate of change of CO$_2$ inside the chamber:

$$F_{CO_2} = \left(\frac{dp_{CO_2}}{dt} \right) \left(\frac{V}{RTS} \right) \tag{3}$$

where dp_{CO_2}/dt is the slope of the gas accumulation in the chamber along time in μatm/s, V is the volume of the chamber (0.23 dm^3), S is the surface area of the chamber (0.33 dm^2), T is the air temperature in Kelvin and R is the ideal gas constant in l atm K^{-1} mol^{-1}. Measurements were randomly distributed within each channel. Note that positive values represent gas efflux to the atmosphere and negative values gas influx from the atmosphere to the water.

2.6 | Data analysis

We used one-way analysis of variance (ANOVA) with blocks as a fixed factor to test for differences among experimental arrays for all variables before treatment onset. Then, differences between time and treatments were assessed with a linear mixed-effect model (LMM) with repeated measures. Treatment, time (different dates) and their interaction were considered as fixed factors, and blocks as a random factor. Variance parameters were estimated using the restricted maximum likelihood estimation method. Artificial streams were considered as subjects and time as a repeated measure factor. The diagonal covariance type matrix was selected among other structures for the repeated measures based on the Akaike information criterion (AIC) and the Schwarz Bayesian information criterion (BIC) (Table S1). Block was not significant in any of the analyses, being therefore removed, and using only treatment and time factors and their interaction to simplify the model. Given that the used statistics were parametric, we checked the normality and homoscedasticity of all variables using the Shapiro–Wilk and Levene tests, respectively. All variables except WEOM fulfilled these conditions, and WEOM was therefore log-transformed. Pairwise comparisons adjusted using the Dunn–Sidak correction were applied to determine differences among the treatment or time means when significantly different effects were found. Finally, to test whether the CO2 emission significantly deviated from 0 (equilibrium with the atmosphere), a one-sample Student's t test was used. All analyses were considered significant at $p < .05$ and were performed with the IBM SPSS Statistics 20 software (SPSS Inc., Chicago, IL, USA).

3 | RESULTS

3.1 | Experimental conditions

Temperature was held constant during the entire experiment and between the different treatments. Thus, air temperature in the

Experimental Streams Facility room averaged 20.6 ± 3.0°C, whereas water temperature in the artificial streams averaged 20.3 ± 1.8°C in all treatments. Photosynthetically active radiation cycles were also steady throughout the experiment, as well as the hydraulics. The non-flow phase involved a progressive decrease in the sediment water content, which decreased down to non-detectable values by day 20 in those treatments under dry conditions (NF, I, RH, Figure 2). The rehydration event involved an increase up to approximately 14% in water content (50% regarding the water content of the F treatment), which again fell down to 2% in a week. Overall, with regard to water content, differences between treatments, dates and the interaction were significant (LMM treatment and date factor, $p < .001$). Pairwise comparisons showed significant differences between all the treatments ($p < .001$) and temporal differences arose from before drying (-1 day) to the end (pairwise comparisons: $p < .05$; Table S1).

3.2 | Water and sediment chemistry

Dissolved oxygen, pH and specific conductivity showed no statistically significant differences between arrays before the onset of the treatments (-1 day, Table 1, Figure S1). Water conductivity slightly increased during the experiment (LMM time factor, $p < .001$) mainly in I and RH after flow recovery (LMM treatment x time interaction, and pairwise comparisons, $p < .001$; Figure S1). Dissolved oxygen was steady throughout the entire experiment and among treatments, with values between 8.9 and 9.8 mg/L. F showed a higher oxygen concentration and lower pH than I and RH (treatment pairwise comparisons: $p < .001$; Table S1) during the experiment (Figure S1).

Nutrients in the water column (N-NH$_4^+$, N-NO$_3^-$ and SRP) showed no significant differences between arrays before the onset of the treatments (-1 day, Table 1). Flow recovery involved an increase in N-NO$_3^-$ and SRP in the treatments I and RH regarding F, but concentrations decreased to similar values in all treatments at the end of the experiment (pairwise comparisons: $p < .01$ for N-NO$_3^-$ and $p < .05$ for SRP; Table S1; Figure S1).

None of the variables describing the quantity or quality of organic matter in either water column (DOC) or sediment (WEOM, HIX and BIX) showed significant differences between arrays before the onset of the treatments (-1 day, Table 1). DOC remained relatively low and constant at the F treatment during the whole experiment, but showed temporal differences in the other treatments. Thus, flow recovery involved high DOC values in the water column in the I and RH treatments (Figure 3a), although the observed values at I were significantly higher than those at RH (t test, $p < .05$). In fact, DOC values returned to basal concentrations two days after flow recovery (LMM time factor, $p < .001$; Table 2). The quantity and composition of WEOM in the sediments significantly responded to the changes in hydrology (LMM treatment and time factors, $p < .001$; Table 2, Figure 3b). Similar to what was described for DOC, WEOM remained low and constant in the F treatment, but showed temporal variation in the other treatments. Specifically, WEOM increased progressively during the non-flow period, but both rehydration and flow recovery involved decreases in WEOM (RH and I treatments). With regard to the quality of organic matter, HIX averaged 0.32 ± 0.10 before treatment implementation (Figure 3c) and BIX averaged 1.08 ± 0.31 (Figure 3d). HIX remained low and only showed a slight increase along the entire experiment at the F treatment, but increased considerably during the non-flow period at the I, RH and NF treatments (LMM treatment and time factors, $p < .001$; Table 2). In contrast, BIX decreased in all treatments along the experiment, indicating the ageing of the biofilms in the artificial streams. However, the changes in BIX were less pronounced than those in HIX, as shown by their lower F values obtained in the LMM (Table 2). Furthermore, the ageing was more pronounced in the I, RH and NF treatments during the non-flow period.
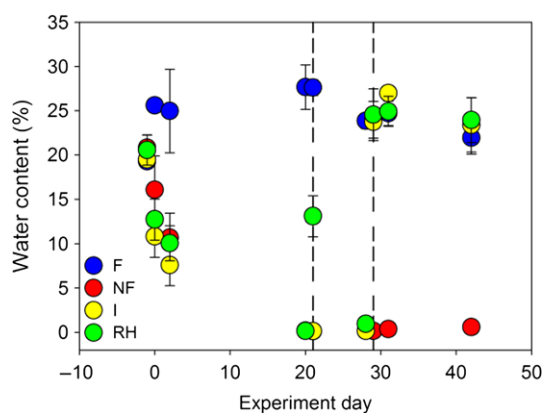

FIGURE 2 Water content (as weight percentage of water in sediment) throughout the experiment and for the different treatments (mean ± standard error, $n = 4$). Note that the first vertical dashed line indicates the moment when the rehydration event occurred (only for RH), whereas the second dashed line indicates flow resumption (only for I and RH) [Colour figure can be viewed at wileyonlinelibrary.com]

TABLE 1 Initial water column and sediment characteristics, and results of the one-way ANOVA (factor: treatment; $n = 16$)

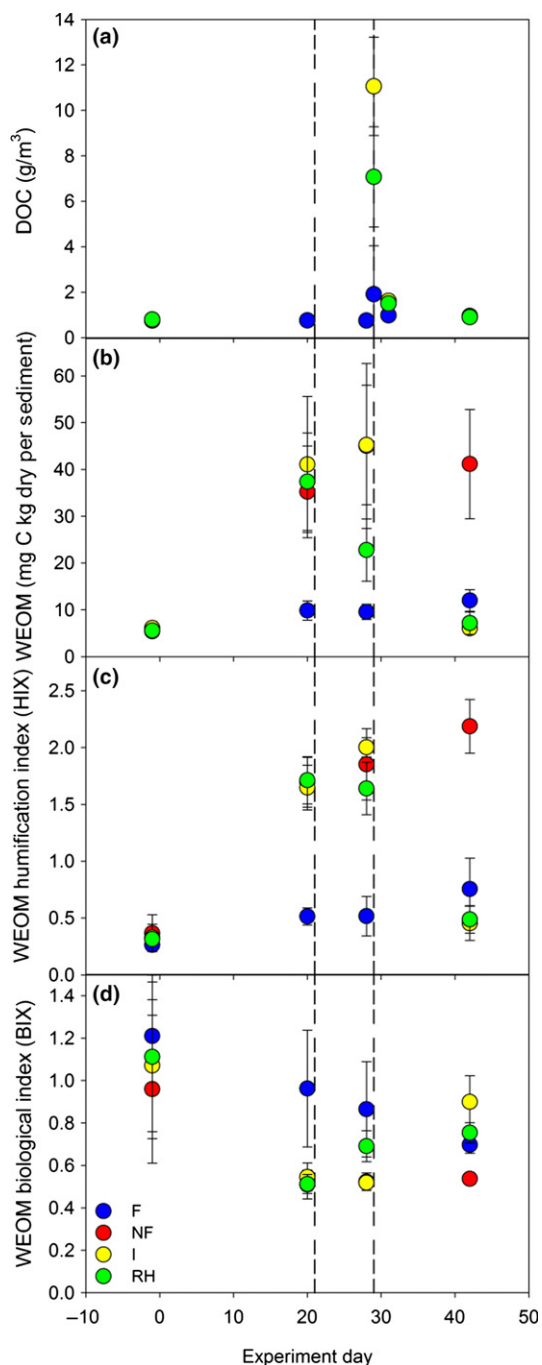|	Mean ± Standard error	F	p
Conductivity (μS/cm)	107.6 ± 0.14	1.34	.31
Redox	214.6 ± 0.96	0.16	.92
Dissolved oxygen (mg/L)	9.51 ± 0.03	0.30	.82
pH	8.02 ± 0.02	0.25	.86
DOC (mg/L)	0.77 ± 0.01	0.46	.71
N-NO$_3^-$ (mg/L)	1.22 ± 0.006	1.84	.08
SRP (mg/L)	0.03 ± 0.001	1.72	.22
WEOM DOC (mg C kg per sediment)	5.76 ± 0.25	0.42	.74
WEOM BIX	1.08 ± 0.08	0.34	.74
WEOM HIX	0.32 ± 0.02	0.73	.56
CO$_2$ flux (μmol m^{-2} day^{-1})	−8.74 ± 0.31	0.14	.93

FIGURE 3 Dissolved organic carbon at the water column (DOC, a), water-extractable organic carbon (WEOM, b), WEOM humification index (HIX, c) and WEOM biological index (BIX, d) along the experiment and for the different treatments (mean ± standard error, $n = 4$). Note that the first vertical dashed line indicates the moment the rehydration event occurred (only for RH), whereas the second dashed line indicates flow resumption (only for I and RH) [Colour figure can be viewed at wileyonlinelibrary.com]

3.3 | Biofilm structure and function

Biofilm variables on structure (F_0, bacterial density) and function (Y_{eff}, APA and LAP) showed no significant differences between arrays before the onset of the treatments (−1 day, Table 1). Thus, F_0

TABLE 2 Summary of the linear mixed-effects model for the variables measured in the experiment. Treatment and date were used as fixed factors

	Treatment		Date		Treatment × Date	
	F	**p**	**F**	**p**	**F**	**p**
DOC	17.86	.001	36.81	<.001	8.53	.001
$N-NO_3^-$	51.36	<.001	57.25	<.001	22.12	<.001
SRP	6.3	.018	23.32	<.001	7.89	.001
WEOM	21.66	<.001	70.90	<.001	14.70	<.001
WEOM HIX	80.50	<.001	208.90	<.001	31.04	<.001
WEOM BIX	5.64	.006	9.18	.001	6.21	.001
F_0	219.63	<.001	66.40	<.001	24.30	<.001
Bacterial density	7.21	<.001	14.90	<.001	2.39	.0401
Y_{eff}	154.44	<.001	262.60	<.001	41.90	<.001
APA	24.77	<.001	2.64	.061	1.72	.120
LAP	72.38	<.001	23.38	<.001	8.28	<.001
CO_2 flux	4.28	.011	90.00	<.001	15.23	<.001

averaged 894 ± 91 before treatment implementation, and bacterial density averaged 4.3 10^8 ± 0.1 10^8 cells/cm². After treatment implementation, F_0 decreased progressively during the non-flow period following the decrease in water content, and did not respond to the rehydration, and showed a slow recovery after the flow recovery (Figure 4a). Differences between treatment, time and the interaction were significant (Table 2). Pairwise comparisons showed significant differences between F and the other treatments ($p < .001$; Table S1). The temporal differences were more evident between the first days of the experiment (before to start the non-flow phase) and the other sampling dates ($p < .01$; Table S1; Figure 4a).

Similarly, bacterial density decreased progressively during the non-flow period, did not respond to the rehydration event and only partially recovered after the flow resumption (Figure 4b). Overall, neither for F_0 nor for bacterial density was there an effect of the non-flow period severity on the observed patterns during the recovery period. There were significant differences in the bacterial number between treatments and dates, but marginally significant for the interaction (Table 2, Figure 4b). Bacterial density in F was significantly higher than in NF and RH (pairwise comparisons: $p < .05$; Table S1) but not in I. The number of bacteria was also higher at the beginning of the experiment just before the start of the non-flow phase in all treatments (pairwise comparisons: day −1 regarding the other dates, $p < .01$; Table S1) and decreased once the experiment started without significant temporal differences.

The photosynthetic efficiency, Y_{eff}, averaged 0.35 ± 0.05 before treatment implementation. The exposure to non-flow conditions involved a decrease in Y_{eff} (Figure 4c), although the decrease was not progressive like for F_0. Instead, Y_{eff} remained unchanged for the first 3 days and then abruptly fell to almost un-detectable levels by day 10. The response to the rehydration pulse was also different than that observed in F_0, as Y_{eff} increased up to approximately 60% of the F values. Y_{eff} also showed a fast recovery with flow recovery, as both I and RH equalled the F treatment 1 day after flow recovery. Differences
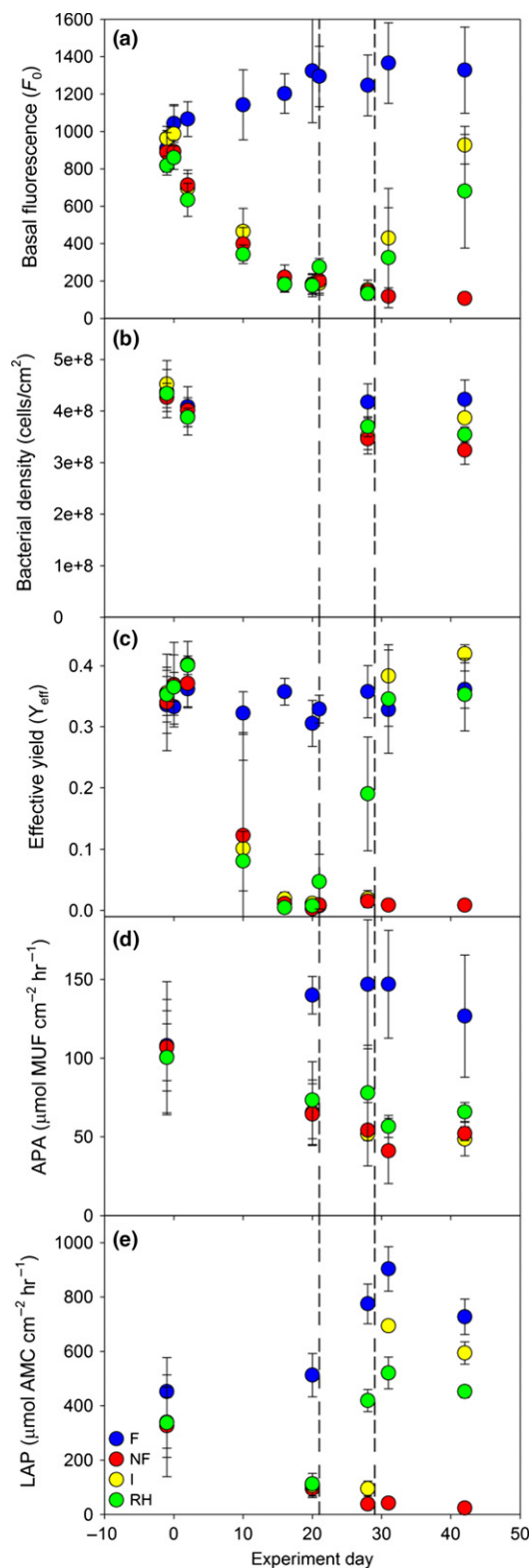
FIGURE 4 Basal fluorescence (F_0, a), bacterial density (DAPI, b), effective yield (Y_{eff}, c), alkaline phosphatase activity (APA, d) and leucine amino peptidase (LAP, e) along the experiment and for the different treatments (mean ± standard error, $n = 4$). Note that the first vertical dashed line indicates the moment the rehydration event occurred (only for RH), whereas the second dashed line indicates flow resumption (only for I and RH) [Colour figure can be viewed at wileyonlinelibrary.com]

between treatments, time and the interaction were significant (LMM treatment and time factors, $p < .001$; Table 2). Pairwise comparisons showed that only RH and I treatments had similar changes. Significant correlations were observed between Y_{eff} and water content in NF ($r = .85$, $p < .05$) and RH ($r = .91$, $p < .05$). Overall, Y_{eff} showed different patterns than F_0, although the recovery after the non-flow period was not influenced by the severity of the period in none of them.

The enzymatic activities before treatment implementation averaged 104 ± 4 µmol MUF cm^{-2} h^{-1} in the case of APA and 363 ± 134 µmol AMC cm^{-2} h^{-1} in the case of LAP. Exposure to non-flow conditions caused both enzymatic activities to decrease, although the effects of rehydration and flow recovery differed among them. Thus, APA only slightly responded to rehydration and showed no response after flow recovery (Figure 4d). In contrast, LAP responded to rehydration with an increase up to 50% of the F values and recovered fast after flow recovery (Figure 4e). Significant differences between treatments, time and the interaction (Table 2) were found. For LAP, NF always showed the lowest values, and F the highest, and both were significantly different from the other treatments and between them (pairwise comparisons: $p < .001$; Table S1). However, the severity of the non-flow period did not influence the patterns observed during the recovery period.

3.4 | CO$_2$ fluxes

The CO$_2$ flux before treatment implementation averaged -4.48 ± 0.50 mmol m^{-2} day^{-1} without significant differences between treatments (Table 1), thus indicating the dominance of uptake over the release of CO$_2$ in the artificial streams. During the entire experiment, the F treatment showed CO$_2$ fluxes close to the equilibrium with the atmosphere (from 0.5 to -10 mmols m^{-2} day^{-1}). In contrast to F, the exposure to non-flow conditions caused an immediate increase in the CO$_2$ influx, indicating a higher uptake rate of CO$_2$ by the artificial streams, which lasted for the first 6 hr (Figure 5). Then, the artificial streams transitioned from uptake to emission of CO$_2$ and remained with similar values during the entire non-flow period till the rehydration pulse, which increased the CO$_2$ flux in RH (pairwise comparisons: 21 days significantly different from the previous dates, $p < .001$), indicating an increase in the release of CO$_2$ that lasted at least 9 hr (Figure 5c; significantly different from 0, t test $p < .05$). A similar increase in the release of CO$_2$ was observed in I and RH treatments with the flow resumption (Figure 5d; significantly different from 0, t test $p < .05$). There were significant differences in CO$_2$ emissions between treatments, time and their interaction (LMM; Table 2). Overall, and similar to what was described above for other biofilm structure and function variables, the severity of the non-flow period did not influence the recovery of the CO$_2$ fluxes after flow resumption.

| DISCUSSION

The exposure of biofilms to non-flow conditions impacted their structure and function. These changes were significant for all
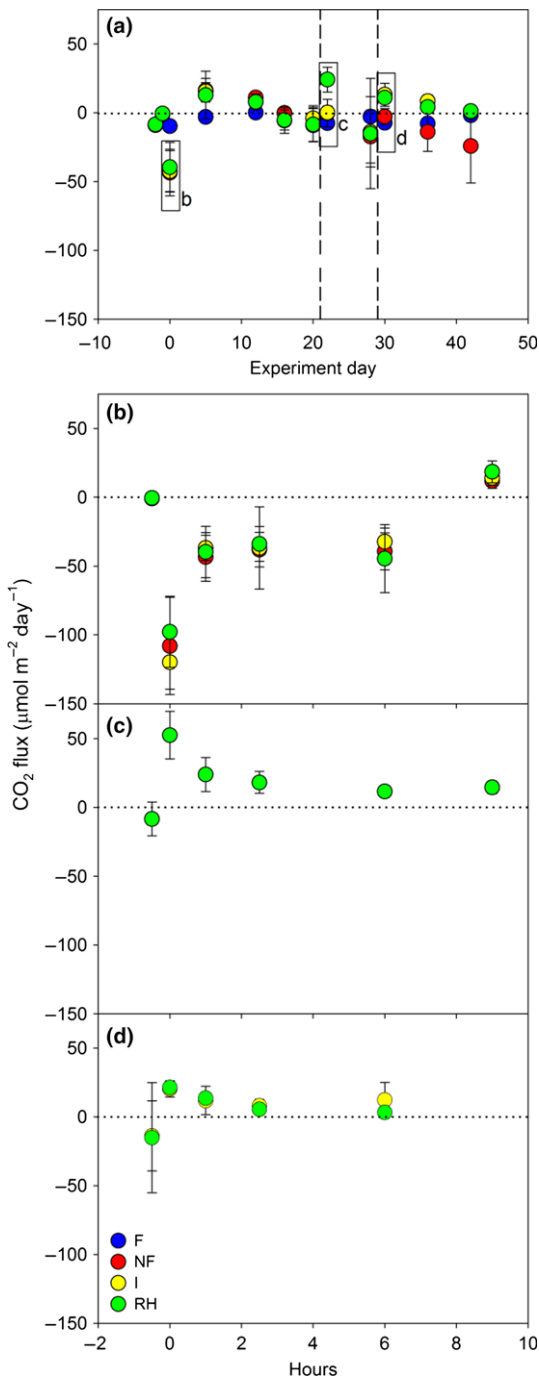
FIGURE 5 CO_2 flux to and from the artificial streams sediments along the experiment and for the different treatments (mean $\pm$ standard error, $n = 4$) (a); CO_2 fluxes on the first day of the non-flow period (treatments NF, I and RH) (b); on the first day after the rehydration event (treatment RH) (c); and on the first day after flow recovery (treatments I and RH), (d). Note that in panel (a), the first vertical dashed line indicates the moment the rehydration event occurred (only for RH), whereas the second dashed line indicates flow resumption (only for I and RH) [Colour figure can be viewed at wileyonlinelibrary.com]

considered variables, although these changes were not equivalent among variables or linear over time. A decoupling between autotrophic structure (F_0) and function (Y_{eff}) was evident, as F_0 steadily

decreased during the non-flow period, whereas Y_{eff} remained unaltered for a few days and then abruptly collapsed. The biomass of primary producers showed a linear response to the duration of the non-flow period, as it steadily decreased during this period, whereas photosynthetic function only decreased after complete desiccation, as has been reported for natural biofilms from temporary streams (Timoner et al., 2012) and for biofilms developed in artificial streams (Acuña et al., 2015).

In regard to CO_2 fluxes, there was a clear transition from net uptake to net release along the non-flow period. Specifically, high net uptake rates were observed during the first 6 hr of the non-flow period, probably caused by the remaining photosynthetic activity (Y_{eff} only decreased after 4 days). After these 6 initial hours, CO_2 release dominated over uptake, although observed values were near the equilibrium with the atmosphere (i.e. fluxes close to 0). Our study adds to the current knowledge by accounting for the pronounced temporal variability of dry streambeds along the non-flow period. The trends uncovered in our manipulative experiments leads us to suggest that dry streambeds may not only be one-way CO_2 emitters, as was previously found in temporally restricted studies (Gómez-Gener et al., 2016) but also environments that host suitable conditions for CO_2 uptake/fixation (i.e. autotrophic dominated biofilms), at least during short periods after flow cessation.

Regarding sediment organic matter quality before the non-flow period, HIX values were relatively low and BIX high if compared with values reported from natural streams, at either the benthos (Gómez-Gener et al., 2016) or the water column (Ejarque et al., 2017), thus indicating a predominance of autochthonous organic matter in the artificial streams. However, non-flow conditions involved significant increases in WEOM and HIX, as well as decreases in BIX. These changes might be explained by several physical, chemical and biological mechanisms acting simultaneously (Borken & Matzner, 2009; Kaiser, Kleber, & Berhe, 2015). Non-flow conditions can strongly modify sediment structure (e.g. by disrupting aggregates) and increase its hydrophobicity, thereby affecting the availability of organic matter. In addition, non-flow conditions can cause bacterial and algal cell death (Timoner et al., 2012), thus releasing additional organic matter to sediment interstitial spaces (Baldwin & Mitchell, 2000). Our results also suggest that the organic matter released from microbial dying organisms (less humic and fresher) was either not enough to compensate this humic organic matter, or it was rapidly humidified by the decomposing activity of surviving microbes during the first days of the non-flow period. In contrast to the artificial streams, field conditions may allow a higher diversity of organic matter, and sometimes larger amounts of stored organic matter in sediments. Furthermore, field conditions might also allow a faster recolonisation after exposure to non-flow conditions because of the likely existence of refugia from non-flow events (Romaní et al., 2013). Therefore, the results from this artificial stream experiment should be cautiously applied to real-world situations. Nevertheless, controlled experimental systems such as the artificial streams eliminate irrelevant variability between treatments and replicates, giving much greater statistical power to identify the effects of interest.

4.1 | Severity effects during the non-flow period

The sediment rehydration resulting from the simulated rainfall event sufficed to affect the biofilm in our artificial streams for around a week. The response was only observed in functional terms, as only photosynthetic (Y_{eff}) and exoenzymatic (LAP) activities increased significantly, while that was not the case of biomass-related variables such as the basal fluorescence F_0 or the bacterial density. However, note that not all functional variables equally responded to the severity of the non-flow period, as APA did not show any differences between treatments RH and I. This decoupling between the enzyme activities APA and LAP did not correspond to differences in the dissolved forms of N and P at the end of the non-flow period, but might be related to differences in the availability and demand of N and P forms for active bacteria during the non-flow period. Responses to rehydration during the non-flow period have rarely been reported in temporary streams, but there are several studies on terrestrial soils (Huxman et al., 2004; Williams, 2007) and at least one in a temporary stream (Timoner, Acuña et al., 2014). Thus, rehydration events are known to significantly increase stream biofilm functional diversity (Timoner, Acuña et al., 2014). Furthermore, the magnitude and frequency of the rain episodes influence the carbon balance of soils in arid lands (Huxman et al., 2004). The response of soil biofilm functioning to rehydration events has been attributed to physiological and functional changes rather than structural changes in communities (Williams, 2007).

The observed changes in biofilm functioning in our artificial streams during the non-flow period after the rehydration event were reflected in higher CO_2 emissions, as well as in lower WEOM. This indicates that a higher frequency of rainfall events might reduce or exhaust the carbon reservoir in dry streambeds, increasing instream organic carbon processing and degassing, and reducing exports during the recovery of flow. However, changes were not only related to the quantity of WEOM but also with the quality. Thus, although changes were not as pronounced as for the quantity, the rehydration caused WEOM HIX to decrease and the WEOM BIX to increase; meaning that the WEOM in the artificial streams experiencing rehydration was less humic (lower HIX values) and fresher. Because of that, differences in the composition of the exported dissolved organic matter after flow resumption could be expected.

The rehydration event induced a net release of CO_2 from the sediment that lasted for approximately 9 hr after the rehydration event. This was most likely caused by the increase in heterotrophic activity (as reflected in exoenzymatic activities, especially LAP). Similar patterns have been observed in the soils (Sponseller, 2007) and dry streambeds (Gallo et al., 2014) of desert catchments after a rehydration pulse; with increases of CO_2 emissions up to 30 times the basal one and lasting for approximately 48 hr (Sponseller, 2007). In this direction, high fluxes following a soil rehydration event have been described as the "Birch effect," a set of biogeochemical responses to a wetting pulse following a period of drought that include the enhanced decomposition of labile soil organic matter, increased rates of nitrogen mineralisation (Birch, 1958) and high

post-wetting CO_2 flux (Austin et al., 2004; Borken & Matzner, 2009; Casals, Lopez-Sangil, Carrara, Gimeno, & Nogués, 2011; Fierer & Schimel, 2003; Jarvis et al., 2007).

4.2 | Severity effects after the non-flow period

We expected severity during the non-flow period to influence the biofilm structure and function after flow recovery, so that a lower severity would result in faster recoveries. However, this was not the case and no relationship was observed between the severity and rate of biofilm recovery. Similarly, some studies in soils also reported no effects of severity on the bacterial communities at the end of the dry period (Fierer & Schimel, 2003; Griffiths et al., 2003). However, there are also studies reporting effects of severity on soil fungi, although not in bacteria (Drenovsky, Vo, Graham, & Scow, 2004). Overall, our results indicate that the severity of the non-flow period in temporary streams does not influence the microbial rate of recovery, or at least not bacterial and algal functional responses.

Regardless of the effects of severity, there was a CO_2 pulse following the flow recovery, which was slightly lower in terms of magnitude and duration to that experienced after the rehydration. Furthermore, almost no WEOM was available after flow recovery, indicating the cleansing of sediments. The remaining WEOM after flow recovery had a more humic and fresh character similar to that of the continuously flowing treatment. These results indicate that WEOM during that period probably almost exclusively consisted of fresh algal exudates.

Our results partially supported the initial hypotheses. Specifically, no apparent changes were detected in terms of the structure between treatments experiencing different levels of severity during the non-flow conditions (rejection of hypothesis i), although biofilm functioning was enhanced by the rehydration pulse, and in some cases maintained high levels till the end of the non-flow period (support of hypothesis ii). With regard to the recovery after the non-flow period, we detected no differences between treatments experiencing different severity levels (rejection of hypothesis iii). This means that the rehydration pulse involved a decoupling between structure and function, as only function responded to rehydration. Thus, the short rehydration pulse was enough to enhance photosynthetic and enzymatic activities, and this led to higher CO_2 emissions and to a lower WEOM. This apparent decoupling between structure and function was also observed at two crucial moments: the first days of the non-flow period, and the flow recovery period. While the structural variables such as F_0 experienced a slow and progressive decrease during the non-flow period, functional variables such as Y_{eff} maintained their activity for few days and then collapsed. The rate of change was also behind the differences during the flow recovery period, as F_0 increased slowly, while Y_{eff} recovered its maximum levels immediately. Interestingly, there was a transition during the non-flow period from an autotrophic CO_2 uptake to a heterotrophic CO_2 release, thus indicating a differential effect of the exposure to non-flow conditions on autotrophs and heterotrophs. Overall, the severity of the

non-flow period did not influence the biofilm structure and function of the artificial streams after the flow recovery, although it influenced the biofilm functioning during the non-flow period and therefore the ecosystem carbon balance, as less severity implied more processing and emissions, and less organic matter availability at the end of the non-flow period. Given the expected climate change-driven changes in the rainfall patterns in arid and semi-arid areas (Polade et al., 2014), we expect longer, harsher and more frequent non-flow periods (Jaeger, Olden, & Pelland, 2014; Pekel et al., 2016). In turn, this might imply higher WEOM values of high humic content, which might be easily exported downstream with the flow onset.

ORCID

Meritxell Abril 🆔 http://orcid.org/0000-0002-5103-5567

Vicenç Acuña 🆔 http://orcid.org/0000-0002-4485-6703

REFERENCES

Acuña, V., Casellas, M., Corcoll, N., Timoner, X., & Sabater, S. (2015). Increasing extent of periods of no flow in intermittent waterways promotes heterotrophy. *Freshwater Biology*, *60*, 1810–1823. https://doi.org/10.1111/fwb.12612

Acuña, V., Datry, T., Marshall, J., Barceló, D., Dahm, C. N., Ginebreda, A., ... Palmer, M. A. (2014). Why should we care about temporary waterways? *Science*, *343*, 1080–1081. https://doi.org/10.1126/science.1246666

Amalfitano, S., Fazi, S., Zoppini, A., Barra Caracciolo, A., Grenni, P., & Puddu, A. (2008). Responses of benthic bacteria to experimental drying in sediments from Mediterranean temporary rivers. *Microbial Ecology*, *55*, 270–279. https://doi.org/10.1007/s00248-007-9274-6

Austin, A. T., Yahdjian, L., Stark, J. M., Belnap, J., Porporato, A., Norton, U., ... Schaeffer, S. M. (2004). Water pulses and biogeochemical cycles in arid and semiarid ecosystems. *Oecologia*, *141*, 221–235. https://doi.org/10.1007/s00442-004-1519-1

Bade, D. L. (2009). Gas exchange at the air – Water interface. In G. Likens (ed), *Encyclopedia of Inland Waters* (pp 70–78). Academic Press.

Baldwin, D. S., & Mitchell, A. M. (2000). The effects of drying and re-flooding on the sediment and soil nutrient dynamics of lowland river-floodplain systems: A synthesis. *Regulated Rivers: Research & Management*, *16*, 457–467. https://doi.org/10.1002/(ISSN)1099-1646

Birch, H. (1958). The effects of soil drying on humus decomposition and nitrogen availability. *Plant and Soil*, *10*, 9–31. https://doi.org/10.1007/BF01343734

Bogan, M. T., Boersma, K. S., & Lytle, D. A. (2013). Flow intermittency alters longitudinal patterns of invertebrate diversity and assemblage composition in an arid-land stream network. *Freshwater Biology*, *58*, 1016–1028. https://doi.org/10.1111/fwb.12105

Borken, W., & Matzner, E. (2009). Reappraisal of drying and wetting effects on C and N mineralization and fluxes in soils. *Global Change Biology*, *15*, 808–824. https://doi.org/10.1111/j.1365-2486.2008.01681.x

Casals, P., Lopez-Sangil, L., Carrara, A., Gimeno, C., & Nogués, S. (2011). Autotrophic and heterotrophic contributions to short-term soil CO 2 efflux following simulated summer precipitation pulses in a Mediterranean dehesa. *Global Biogeochemical Cycles*, *25*, 1–12.

Casas-Ruiz, J. P., Catalán, N., Gómez-Gener, L., von Schiller, D., Obrador, B., Kothawala, D. N., ... Marcé, R. (2017). A tale of pipes and reactors: Controls on the in-stream dynamics of dissolved organic matter in rivers. *Limnology & Oceanography*, *62*(S1), S85–S94. https://doi.org/10.1002/lno.10471

Colls, M., Timoner, X., Sabater, S., & Acuña, V. (2018). Effects of duration and frequency of the non-flow period on stream metabolism. *Global Change Biology*. In revision.

Corcoll, N., Casellas, M., Huerta, B., Guasch, H., Acuña, V., Rodríguez-Mozaz, S., ... Sabater, S. (2015). Effects of flow intermittency and pharmaceutical exposure on the structure and metabolism of stream biofilms. *The Science of the Total Environment*, *503–504*, 159–170. https://doi.org/10.1016/j.scitotenv.2014.06.093

Davis, J., Pavlova, A., Thompson, R., & Sunnucks, P. (2013). Evolutionary refugia and ecological refuges: Key concepts for conserving Australian arid zone freshwater biodiversity under climate change. *Global Change Biology*, *19*, 1970–1984. https://doi.org/10.1111/gcb.12203

Doering, M., Uehlinger, U. R. S., Ackermann, T., & Woodtli, M. (2011). Spatiotemporal heterogeneity of soil and sediment respiration in a river-floodplain mosaic (Tagliamento, NE Italy). *Freshwater Biology*, *56*, 1297–1311. https://doi.org/10.1111/j.1365-2427.2011.02569.x

Drenovsky, R. E., Vo, D., Graham, K. J., & Scow, K. M. (2004). Soil water content and organic carbon availability are major determinants of soil microbial community composition. *Microbial Ecology*, *48*, 424–430. https://doi.org/10.1007/s00248-003-1063-2

Ejarque, E., Freixa, A., Vazquez, E., Guarch, A., Amalfitano, S., Fazi, S., ... Butturini, A. (2017). Quality and reactivity of dissolved organic matter in a Mediterranean river across hydrological and spatial gradients. *Science of the Total Environment*, *599–600*, 1802–1812. https://doi.org/10.1016/j.scitotenv.2017.05.113

Febria, C. M., Hosen, J. D., Crump, B. C., Palmer, M. A., & Williams, D. D. (2015). Microbial responses to changes in flow status in temporary headwater streams: A cross-system comparison. *Frontiers in Microbiology*, *6*, 522.

Fierer, N., & Schimel, J. P. (2003). A proposed mechanism for the pulse in carbon dioxide production commonly observed following the rapid rewetting of a dry soil. *Soil Science Society of America Journal*, *67*, 798. https://doi.org/10.2136/sssaj2003.0798

Gallo, E. L., Lohse, K. A., Ferlin, C. M., Meixner, T., & Brooks, P. D. (2014). Physical and biological controls on trace gas fluxes in semi-arid urban ephemeral waterways. *Biogeochemistry*, *121*, 189–207. https://doi.org/10.1007/s10533-013-9927-0

Garcia, C., Gibbins, C. N., Pardo, I., & Batalla, R. J. (2017). Long term flow change threates invertebrate diversity in temporary streams: Evidence from an island. *Science of the Total Environment*, *580*, 1453–1549. https://doi.org/10.1016/j.scitotenv.2016.12.119

Genereux, D. P., & Hemond, H. F. (1992). Determination of Gas exchange rate constants for a small stream on Walker Branch Watershed, Tennessee. *Water Resources Research*, *28*, 2365–2374. https://doi.org/10.1029/92WR01083

Gómez-Gener, L., Obrador, B., Marcé, R., Acuña, V., Catalán, N., Casas-Ruiz, J. P., ... von Schiller, D. (2016). When water vanishes: Magnitude and regulation of carbon dioxide emissions from dry temporary streams. *Ecosystems*, *19*, 710–723. https://doi.org/10.1007/s10021-016-9963-4

Griffiths, R. I., Whiteley, A. S., Anthony, G., Donnell, O., Bailey, M. J., & Donnell, A. G. O. (2003). Physiological and community responses of established grassland bacterial populations to water stress. *Applied and Environmental Microbiology*, 69, 6961–6968. https://doi.org/10.1128/AEM.69.12.6961-6968.2003

Hermoso, V., Ward, D. P., & Kennard, M. J. (2013). Prioritizing refugia for freshwater biodiversity conservation in highly seasonal ecosystems. *Diversity and Distributions*, 19, 1031–1042. https://doi.org/10.1111/ddi.12082

Huguet, A., Vacher, L., Relexans, S., Saubusse, S., Froidefond, J. M., & Parlanti, E. (2009). Properties of fluorescent dissolved organic matter in the Gironde Estuary. *Organic Geochemistry*, 40, 706–719. https://doi.org/10.1016/j.orggeochem.2009.03.002

Huxman, T. E., Snyder, K. A., Tissue, D., Leffler, A. J., Ogle, K., Pockman, W. T., ... Schwinning, S. (2004). Precipitation pulses and carbon fluxes in semiarid and arid ecosystems. *Oecologia*, 141, 254–268. https://doi.org/10.1007/s00442-004-1682-4

Indermaur, L., Schmidt, B. R., Tockner, K., & Schaub, M. (2010). Spatial variation in abiotic and biotic factors in a floodplain determine anuran body size and growth rate at metamorphosis. *Oecologia*, 163, 637–649. https://doi.org/10.1007/s00442-010-1586-4

Jaeger, K. L., Olden, J. D., & Pelland, N. A. (2014). Climate change poised to threaten hydrologic connectivity and endemic fishes in dryland streams. *Proceedings of the National Academy of Sciences of the United States of America*, 111 (38), 13894–13899.

Jarvis, P., Rey, A., Petsikos, C., Wingate, L., Rayment, M., Pereira, J., ... Manca, G. (2007). Drying and wetting of Mediterranean soils stimulates decomposition and carbon dioxide emission: The "Birch effect". *Tree Physiology*, 27, 929–940. https://doi.org/10.1093/treephys/27.7.929

Kaiser, M., Kleber, M., & Berhe, A. A. (2015). How air-drying and rewetting modify soil organic matter characteristics: An assessment to improve data interpretation and inference. *Soil Biology and Biochemistry*, 80, 324–340. https://doi.org/10.1016/j.soilbio.2014.10.018

Livingston, G. P., & Hutchinson, G. L. (1995). Enclosure-based measurements of trace gas exchange applications and sources of errors. In P. A. Matson, & R. C. Harris (Eds.), *Methods in ecology. Biogenic trace gases: Measuring emissions from soil and water* (pp. 14–51). Malden, MA: Blackwell Publishing Ltd.

Millero, F. J. (1995). Thermodynamics of the carbon dioxide system in the ocean. *Geochimica et Cosmochimica Acta*, 59, 661–677. https://doi.org/10.1016/0016-7037(94)00354-O

Pekel, J.-F., Cottam, A., Gorelick, N., & Belward, A. S. (2016). High-resolution mapping of global surface water and its long-term changes. *Nature*, 540, 418–422.

Polade, S. D., Pierce, D. W., Cayan, D. R., Gershunov, A., & Dettinger, M. D. (2014). The key role of dry days in changing regional climate and precipitation regimes. *Scientific Reports*, 4, 8.

Raymond, P. A., Hartmann, J., Lauerwald, R., Sobek, S., McDonald, C., Hoover, M., ... Kortelainen, P. (2013). Global carbon dioxide emissions from inland waters. *Nature*, 503, 355–359. https://doi.org/10.1038/nature12760

Raymond, P. A., Zappa, C. J., Butman, D., Bott, T. L., Potter, J., Mulholland, P., ... Newbold, D. (2012). Scaling the gas transfer velocity and hydraulic geometry in streams and small rivers. *Limnology & Oceanography: Fluids & Environments*, 2, 41–53.

Romaní, A. M., Amalfitano, S., Artigas, J., Fazi, S., Sabater, S., Timoner, X., ... Zoppini, A. (2013). Microbial biofilm structure and organic matter use in mediterranean streams. *Hydrobiologia*, 719, 43–58. https://doi.org/10.1007/s10750-012-1302-y

Romaní, A. M., Giorgi, A., Acuña, V., & Sabater, S. (2004). The influen of substratum type and nutrient supply on biofilm organic matter lization in streams. *Limnology & Oceanography*, 49, 1713–17 https://doi.org/10.4319/lo.2004.49.5.1713

Schmitt-Jansen, M., & Altenburger, R. (2008). Community-level microalgal toxicity assessment by multiwavelength-excitation PAM fluorometry. *Aquatic Toxicology*, 86, 49–58. https://doi.org/10.1016/j.aquatox.2007.10.001

Schreiber, U., Müller, J. F., Haugg, A., & Gademann, R. (2002). New type of dual-channel PAM chlorophyll fluorometer for highly sensitive water toxicity biotests. *Photosynthesis Research*, 74, 317–330. https://doi.org/10.1023/A:1021276003145

Schriever, T. A., Bogan, M. T., Boersma, K. S., Cañedo-argüelles, M., Jaeger, K. L., Olden, J. D., & Lytle, D. A. (2015). Hydrology shapes taxonomic and functional structure of desert stream invertebrate communities. *Freshwater Science*, 34, 399–409. https://doi.org/10.1086/680518

Sponseller, R. A. (2007). Precipitation pulses and soil CO2 flux in a Sonoran Desert ecosystem. *Global Change Biology*, 13, 426–436. https://doi.org/10.1111/j.1365-2486.2006.01307.x

Stubbington, R., Gunn, J., Little, S., Worrall, T. P., & Wood, P. J. (2016). Macroinvertebrate seedbank composition in relation to antecedent duration of drying and multiple wet-dry cycles in a temporary stream. *Freshwater Biology*, 61, 1293–1307. https://doi.org/10.1111/fwb.12770

Teodoru, C. R., Prairie, Y. T., & del Giorgio, P. A. (2011). Spatial heterogeneity of surface CO2 fluxes in a newly created eastmain-1 reservoir in Northern Quebec, Canada. *Ecosystems*, 14, 28–46. https://doi.org/10.1007/s10021-010-9393-7

Timoner, X., Acuña, V., Frampton, L., Pollard, P., Sabater, S., & Bunn, S. E. (2014). Biofilm functional responses to the rehydration of a dry intermittent stream. *Hydrobiologia*, 727, 185–195. https://doi.org/10.1007/s10750-013-1802-4

Timoner, X., Acuña, V., von Schiller, D., & Sabater, S. (2012). Functional responses of stream biofilms to flow cessation, desiccation and rewetting. *Freshwater Biology*, 57, 1565–1578. https://doi.org/10.1111/j.1365-2427.2012.02818.x

Timoner, X., Borrego, C. M., Acuña, V., & Sabater, S. (2014). The dynamics of biofilm bacterial communities is driven by flow wax and wane in a temporary stream. *Limnology and Oceanography*, 59, 2057–2067. https://doi.org/10.4319/lo.2014.59.6.2057

Tonolla, D., Acuña, V., Uehlinger, U., Frank, T., & Tockner, K. (2010). Thermal heterogeneity in river floodplains. *Ecosystems*, 13, 727–740. https://doi.org/10.1007/s10021-010-9350-5

Wanninkhof, R. (1992). Relationship between wind speed and gas exchange. *Journal of Geophysical Research*, 97, 7373–7382. https://doi.org/10.1029/92JC00188

Weiss, R. F. (1974). Carbon dioxide in water and seawater: The solubility of a non-ideal gas. *Marine Chemistry*, 2, 203–215. https://doi.org/10.1016/0304-4203(74)90015-2

Welter, J. R., Fisher, S. G., & Grimm, N. B. (2005). Nitrogen transport and retention in an arid land watershed: Influence of storm characteristics on terrestrial-aquatic linkages. *Biogeochemistry*, 76, 421–440. https://doi.org/10.1007/s10533-005-6997-7

Williams, M. A. (2007). Response of microbial communities to water stress in irrigated and drought-prone tallgrass prairie soils. *Soil Biology and Biochemistry*, 39, 2750–2757. https://doi.org/10.1016/j.soilbio.2007.05.025

Williams, M. A., & Rice, C. W. (2007). Seven years of enhanced water availability influences the physiological, structural, and functional attributes of a soil microbial community. *Applied Soil Ecology*, 35, 535–545. https://doi.org/10.1016/j.apsoil.2006.09.014

Wilson, H. F., & Xenopoulos, M. A. (2009). Effects of agricultural land use on the composition of fluvial dissolved organic matter. *Nature Geoscience*, 2, 37–41. https://doi.org/10.1038/ngeo391

olnay, A. (1996). Dissolved humus in soil waters. *Humic Substances in Terrestrial Ecosystems*, 171–223. https://doi.org/10.1016/B978-044481516-3/50005-0

Zsolnay, A., Baigar, E., Jimenez, M., Steinweg, B., & Saccomandi, F. (1999). Differentiating with fluorescence spectroscopy the sources of dissolved organic matter in soils subjected to drying. *Chemosphere*, *38*, 45–50. https://doi.org/10.1016/S0045-6535(98)00166-0

SUPPORTING INFORMATION

Additional Supporting Information may be found online in the supporting information section at the end of the article.